Contribution from the Baker Laboratory of Chemistry,
Cornell University, Ithaca, New York 14853

Chalcogen Ordering on Special-Position Sites in Ternary Molybdenum Chalcogenides

DAVID C. JOHNSON, JEAN-MARIE TARASCON, and M. J. SIENKO*

Received February 1, 1983

The effect on crystallographic parameters of selenium-for-sulfur replacement has been studied in several series of ternary molybdenum chalcogenides of the Chevrel-phase type. In all the systems examined—$MMo_6(S_{1-x}Se_x)_8$ with M = La, Sm, Eu, Yb, Pb, or Ag and $0 < x < 1$—the hexagonal c/a ratio shows a minimum when plotted against the percent sulfur replaced. The minimum is shallowest for the case of Ag and deepest for the case of La. The apparent cause of the minimum is a strong preference by the selenium for occupancy of the general-position chalcogen site rather than the special-position site on the 3 axis. The preferred site ordering is greater for M^{3+} than for M^{2+} or M^+. Delocalization of M off the 3 axis decreases the ordering, as it tends to increase the bonding in the a direction.

Introduction

One of the great challenges in solid-state chemistry is to fine-tune the electronic properties of advanced materials by making selective changes in chemical composition. Among the materials extensively subjected to this kind of study are the Chevrel phases, ternary molybdenum chalcogenides of formula MMo_6X_8. They are of special interest because, depending on M, they may be high-temperature superconductors with extraordinarily high critical fields needed to quench the superconductivity.[1] Attempts to improve the properties by chemical manipulation have generated a large body of crystallographic data out of which interesting new correlations are becoming apparent. Particularly intriguing is the effect on structural parameters of disorder in the occupancy of the chalcogen site. In this investigation we examine systematically several series of Chevrel phases to see the effect of disorder as we replace sulfur by selenium on the chalcogen site positions.

The main building block of the Chevrel phases is the Mo_6X_8 unit in which a distorted cube is formed by eight chalcogen atoms at the cube corners and six molybdenum atoms slightly above the face centers. Individual Mo_6X_8 units are rotated approximately 25° about the 3 axis of the cube so as to optimize the distance between the chalcogen atom of one cube and the molybdenum atom of an adjacent cube. The M atoms are positioned between Mo_6X_8 units either on the 3 axis or in a double belt of 12 tetrahedral sites around this position.

There are two types of chalcogen positions: the two cube corners that are on the 3 axis and the other six cube corners that swing around the 3 axis. The former are referred to as special positions; the latter, as general positions. In mixed chalcogenides, there is evidently the possibility of sorting out the chalcogens between the two positions. A previous study of the $PbMo_6(S_{1-x}Se_x)_8$ system[2] suggested that the selenium atoms preferentially occupy the general positions. The postulate was offered in order to explain why, in the selenium-for-sulfur replacement, the hexagonal c axis (which is directed along 3) rises first slowly and then more rapidly, whereas the a axis (perpendicular to 3) increases more rapidly at first and then more slowly. In this investigation we have examined five other series of $MMo_6(S_{1-x}Se_x)_8$, where M = La, Sm, Eu, Yb, and Ag, to see how the selenium preference for the general-position sites is affected by change in the ternary element M. Data for the Yb and Eu series were obtained from the literature; data for the others were obtained by synthesis of the corresponding phases followed by X-ray examination of the products.

Experimental Section

Sample Preparation. The required phases were prepared from ultrapure starting elements, purity and sources of which are shown in Table I. Prior to use, the molybdenum powder was reduced at 1000 °C under a flow of hydrogen and stored in a vacuum desiccator until needed.

Table I. Starting Materials for $MMo_6(S_{1-x}Se_x)_8$ Synthesis

element	purity, %	source
sulfur	99.9999	Atomergic Chemetals Corp.
selenium	99.9999	Atomergic Chemetals Corp.
molybdenum	99.95	United Mineral and Chemical Corp.
lanthanum	99.99	United Mineral and Chemical Corp.
samarium	99.99	United Mineral and Chemical Corp.
europium	99.99	United Mineral and Chemical Corp.
silver	99.999	Materials Research Corp.

Appropriate amounts of the elements to form 1-g samples of $MMo_6(S_{1-x}Se_x)_8$ (x = 0–1 in 10 steps) were placed in previously degassed silica tubes, which were degassed again at 10^{-6} torr and sealed. All the tubes were placed together in a box furnace, the temperature of which was uniformly and slowly raised to 1050 °C over the course of 5 days. After 24 h at 1050 °C, the samples were cooled in air and vigorously shaken so as to homogenize. They were immediately reheated to 1100 °C, kept there for 48 h, and then air-cooled. The samples were opened in a helium Dri-lab and thoroughly ground. After being resealed in new degassed silica ampules, which in turn were sealed in larger ones, the samples were heated as previously described. The samples were then heated at 1220 °C for 96 h and finally air-cooled.

Powder X-ray Diffraction. X-ray diffraction photographs were made by using a 114.6-mm diameter Debye–Scherrer camera with nickel-filtered Cu Kα radiation. Lines were indexed with the aid of a Fortran program that calculated the positions and intensities of possible reflections from available single-crystal data. A least-squares fit, with corrections for absorption and camera-radius error, was performed by using all lines with θ (hkl) > 30° that could be indexed unambiguously. The procedure yields lattice parameters with errors of less than 1 part per thousand.

Results and Discussion

The X-ray data on the mixed chalcogen systems $MMo_6(S_{1-x}Se_x)_8$ indicated that the bulk samples were all single phased over the whole range of composition $0 < x < 1$. All the lines could be indexed to the appropriate rhombohedral phase. Table II shows the crystal data in detail for the lanthanum system. a_R and α_R are the rhombohedral cell parameters; a_H and c_H are the hexagonal cell parameters. V is the volume of the unit cell. The second series at the bottom of the table represents an independent set of syntheses. It gives an idea of the reproducibility of the measurements.

A plot of unit-cell volume vs. composition for the lanthanum case (Figure 1a) shows a slight negative deviation from Vegard's law. Usually this means one has a valence change or the system is ordering. As it is unlikely that lanthanum is anything but trivalent in all these phases, it must be that the system is ordering. As can be seen from parts b and c of Figure 1, which show the hexagonal cell parameters plotted vs. composition, two straight lines can be drawn to fit the data, one from $x = 0$ to $x = 0.7$ and another, of different slope, from

(1) For reviews of the Chevrel phases see: Yvon, K. *Curr. Top. Mater. Sci.* **1979**, *3*, 53. Fischer, O. *Appl. Phys.* **1978**, *16*, 1.
(2) Delk, F. S., II; Sienko, M. J. *Inorg. Chem.* **1980**, *19*, 1352.

0020-1669/83/1322-3773$01.50/0

Table II. Crystal Data for $LaMo_6(S_{1-x}Se_x)_8$

x	a_R, Å	α_R, deg	a_H, Å	c_H, Å	c/a	V, Å^3
			First Series			
0	6.525 (1)	88.71 (1)	9.123 (2)	11.553 (2)	1.2663 (5)	277.6 (2)
0.1	6.552 (1)	88.90 (1)	9.177 (2)	11.564 (1)	1.2601 (4)	281.1 (2)
0.2	6.575 (1)	89.04 (1)	9.220 (2)	11.578 (2)	1.2557 (4)	284.2 (2)
0.3	6.588 (1)	89.12 (1)	9.245 (2)	11.584 (2)	1.2531 (5)	285.8 (2)
0.4	6.611 (1)	89.32 (1)	9.293 (1)	11.586 (2)	1.2466 (3)	288.8 (1)
0.5	6.641 (1)	89.47 (1)	9.348 (2)	11.609 (1)	1.2418 (4)	292.9 (2)
0.6	6.662 (1)	89.60 (1)	9.388 (2)	11.619 (1)	1.2376 (4)	295.6 (1)
0.7	6.683 (2)	89.74 (2)	9.430 (3)	11.629 (3)	1.2331 (8)	298.5 (3)
0.8	6.709 (1)	89.58 (1)	9.453 (2)	11.703 (1)	1.2382 (3)	301.9 (1)
0.9	6.750 (1)	89.00 (1)	9.462 (1)	11.893 (1)	1.2569 (3)	307.4 (1)
1.0	6.777 (1)	88.57 (1)	9.463 (2)	12.027 (1)	1.2709 (4)	310.9 (1)
			Second Series			
0	6.526 (1)	88.71 (1)	9.126 (1)	11.555 (1)	1.2662 (3)	277.8 (1)
0.7	6.685 (1)	89.74 (1)	9.432 (2)	11.632 (2)	1.2332 (5)	298.7 (2)
1.0	6.776 (1)	88.58 (1)	9.463 (1)	12.023 (2)	1.2706 (4)	310.8 (1)

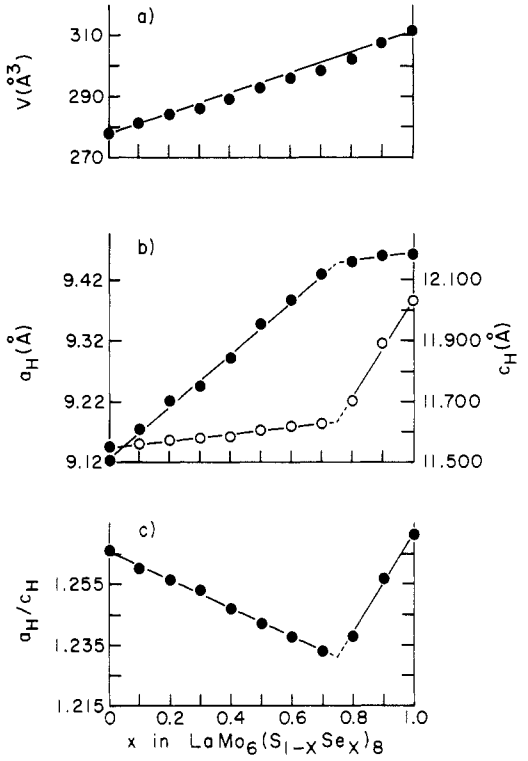

Figure 1. Crystallographic parameters as a function of composition in the series $LaMo_6(S_{1-x}Se_x)_8$. V is the unit-cell volume. a_H (solid circles) and c_H (open circles) are the axial lengths for the hexagonal unit cell. The size of the data points exceeds the error in the fitted values.

$x = 0.8$ to $x = 1.0$. It is interesting to note that the lines cross at the composition $x = 0.75$, which corresponds to $LaMo_6S_2Se_6$, i.e., a completely ordered system in which the two sulfur atoms are in the 3 special positions and the six selenium atoms are in the general positions.

Assuming a hard-sphere, idealized structure, we can calculate the dependence of the c parameter on compositions for the case of complete ordering. The c parameter can be decomposed into the sum of the length of the body diagonal of the chalcogen cube and twice the distance from ternary element to special-position chalcogen. For $y < 6$ in the formulation $LaMo_6S_{8-y}Se_y$, the c parameter is given by eq 1, where

$$c = 2r_{La} + 2r_S + 2(3^{1/2})[(6 - y)r_S + yr_{Se}]/6 \quad (1)$$

r_{La}, r_S, and r_{Se} are, respectively, the radii of lanthanum, sulfur, and selenium atoms. Equation 1 assumes that only sulfur atoms are in the special positions and the size of the chalcogen cube is fixed by the weighted average of the chalcogen radii in the general positions. For $y > 6$, c is given by eq 2. The two equations become identical for $y = 6$.

$$c = 2r_{La} + 2[(8 - y)r_S + (y - 6)r_{Se}]/2 + 2(3^{1/2})r_{Se} \quad (2)$$

For the formulation $LaMo_6(S_{1-x}Se_x)_8$, the composition parameter x is given by $y/8$. Making this substitution in eq 1 and 2 and differentiating with respect to the composition parameter, we get for $x < 0.75$

$$dc/dx = 8(3^{1/2}/3)[r_{Se} - r_S] \quad (3)$$

and for $x > 0.75$

$$dc/dx = 8[r_{Se} - r_S] \quad (4)$$

Clearly, the slope of the c parameter should increase as soon as selenium atoms start to replace sulfur in the special positions. The above model is highly idealized so we should not attach much quantitative significance to the numbers, but it is interesting to note that if we substitute accepted radii for sulfide (1.84 Å) and selenide (1.98 Å), we predict $dc/dx = 0.65$ for $x < 0.75$ and $dc/dx = 1.12$ for $x > 0.75$. The observed values are 0.11 and 1.6, respectively. If the sulfur and selenium were distributed completely at random over the general- and special-position sites for the whole range of concentration, we would expect a continuous increase in c given by $dc/dx = 2 + 2(3^{1/2})(r_{Se} - r_S) = 0.76$.

What happens now when we go to ternary elements other than lanthanum? Figures 2 and 3 summarize the crystallographic parameter changes observed in this investigation upon selenium-for-sulfur replacement in Chevrel phases containing samarium and silver, respectively. It should be noted in the samarium series that the nominal composition for the preparations was $M_{1.2}Mo_6(S_{1-x}Se_x)_8$. Choice of this composition was dictated by indications in the literature[3] that, for the later rare-earth molybdenum chalcogenides, an excess of rare earth should be present to ensure formation of the Chevrel-phase structure. Although all our samples were single phased by X-ray analysis, a magnetic and magnetic resonance study of the europium series (which will be described elsewhere[4]) clearly suggests presence of trace second phase. As these second phases do not affect our site disorder conclusion, we can study the effect of selenium-for-sulfur replacement even in the

(3) Fischer, O.; Treyvaud, A.; Chevrel, R.; Sergent, M. *Solid State Commun.* **1975**, *17*, 721.
(4) Tarascon, J.-M.; Harrison, M. R.; Johnson, D. C.; Sienko, M. J., to be submitted for publication.

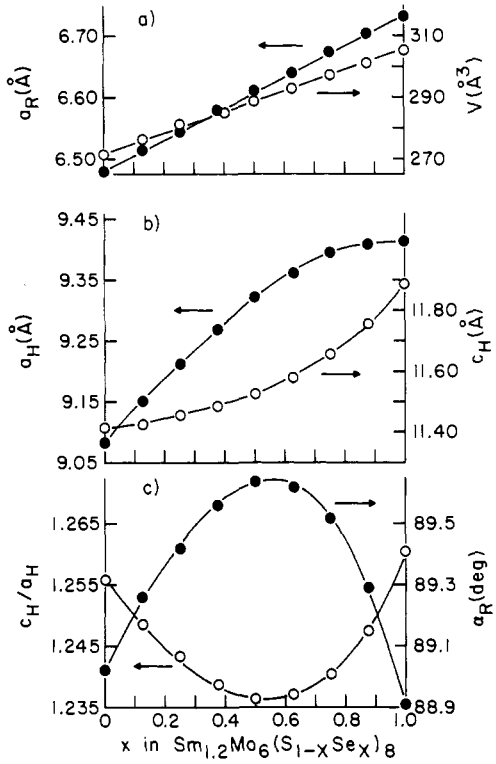

Figure 2. Crystallographic parameters as a function of composition in the series $Sm_{1.2}Mo_6(S_{1-x}Se_x)_8$. Designations are as in Figures 1 and 3.

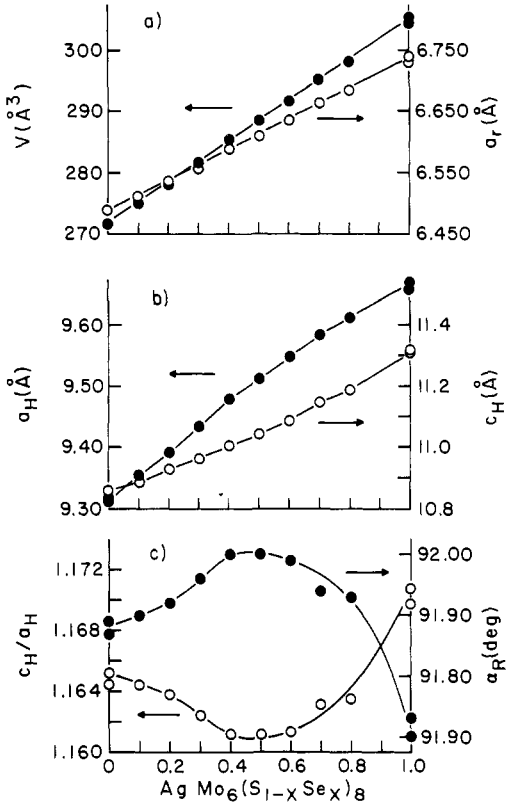

Figure 3. Crystallographic parameters as a function of composition in the series $AgMo_6(S_{1-x}Se_x)_8$. a_H and c_H are the hexagonal cell parameters; a_R and α_R are the parameters for a rhombohedral unit cell.

presence of excess stoichiometric europium or samarium.

Figure 2, for samarium, shows Vegard law behavior in that the unit-cell volume is strictly linear with composition on selenium-for-sulfur replacement. Also, although the a_H parameter again rises more steeply at first than the c_H parameter but subsequently the c_H parameter increases faster, there is apparently no sharp break at $x = 0.75$ as with the lanthanum. We take this to mean that the ordering preference of selenium for general sites rather than special sites is not perfect. There is still some preference for avoiding the 3 axis; otherwise, the two slopes da_H/dx and dc_H/dx would not change as much with composition but apparently there is enough chalcogen mixing to wash out the discontinuity between the two extreme regimes.

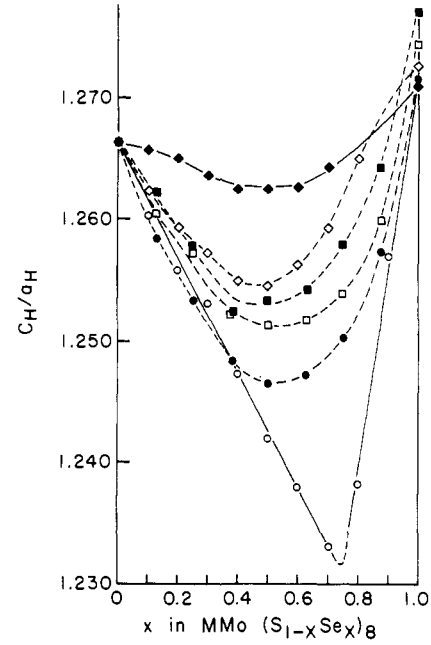

Figure 4. Effect of changing the ternary element M in $MMo_6(S_{1-x}Se_x)_8$ on the course of the composition dependence of the hexagonal crystal parameter ratio c_H/a_H: ♦, Ag; ◇, Pb; ■, Yb; □, Eu; ●, Sm; ○, La. The vertical scale applies to the case where M = La. For the other sysems, the scale has been shifted so the actual c_H/a_H value for MMo_6S_8 coincides with the La case.

Figure 3, for silver, shows even less selenium preference for the general-position chalcogen site resulting in a washed-out transition between general- and special-position occupancy. Another point to note is that in both Figures 2 and 3 the minimum in the c_H/a_H vs. x curve occurs at $x \approx 0.5$, whereas for lanthanum the minimum is clearly at $x = 0.75$.

As c/a vs. x seems to be the most telling indicator for the chalcogen ordering, we have compared the course of the c/a parameter for the six systems for which we now have complete data, viz. $MMo_6(S_{1-x}Se_x)_8$ with M = La, Eu, Sm, Yb, Pb, and Ag. The data for ytterbium were taken from our previous work,[5] for lead, from that of Delk,[2] and for europium, from work to be published.[6] Figure 4 compares the six systems. In each case, as selenium replaces sulfur, the c/a ratio goes through a minumum: the minimum is shallowest for the case of silver, and it is deepest for the case of lanthanum. The depth of the minimum increases in the order Ag^+, Pb^{2+}, Yb^{2+}, Eu^{2+}, Sm^{2+}, La^{3+}. The correlation is with increasing ionic charge, but not with size, as the ionic radii are 1.15, 1.19, 1.02, 1.17, 1.17, and 1.03 Å, respectively. Although less certain, it also appears that the minimum moves from $x = 0.5$ to $x = 0.75$ as the ternary element charge increases from 1+ to 3+.

We propose that the apparent chalcogen ordering that preferentially puts the sulfur on the special-position sites is esssentially a Coulombic effect. Sulfur is smaller and more electronegative than selenium so it effectively puts a larger negative charge closer to the ternary element when the ternary

(5) Tarascon, J.-M.; Johnson, D. C.; Sienko, M. J. *Inorg. Chem.* **1982**, *21*, 1505.
(6) Johnson, D. C., private communication.

element is large and itself sits on the 3 axis. This Coulombic effect would be largest for ternary element M^{3+} and smallest for M^{+}. Therefore, we find La^{3+} producing more chalcogen ordering than does Ag^{+}.

A further point to consider is that, as pointed out by Yvon,[7] the ternary element M may be "delocalized" off the 3 axis, i.e., show large mean-square displacement in directions perpendicular to the 3 axis. This delocalization is favored for small ions such as Cu^{+}, but apparently it is also appreciable for highly polarizable ions such as Ag^{+}. In any case, it is believed that delocalization acts to decrease the chalcogen ordering, as it diminishes the M^{n+} special-position interaction while enhancing the M^{n+} general-position interaction.

A final point to note from Figure 4 is that, aside from the data for Ag^{+} and La^{3+}, the rest of the data roughly cluster together as would be appropriate if all the other ternary elements involved were divalent. This is certainly true for lead[2] and ytterbium.[5] For europium, Mössbauer data[8] reveal a well-defined Eu^{2+} resonance down to 0.5 K. For samarium, the question is still open. It is generally assumed that samarium in these Chevrel phases is trivalent, but these crystallographic data suggest that it is divalent. Magnetic susceptibility studies now in progress should give an unequivocal answer to the question.

Acknowledgment. This research was sponsored by the Air Force Office of Scientific Research through Grant No. 80-0009 and was supported in part by the National Science Foundation and the Materials Science Center at Cornell University.

(7) Yvon, K. *Solid State Commun.* **1978**, *25*, 327.

(8) Fradin, F. Y.; Shenoy, G. K.; Dunlap, B. D.; Aldred, A. T.; Kimball, K. C. *Phys. Rev. Lett.* **1977**, *38*, 719.

Contribution from the Department of Chemistry, University of California, Berkeley, California 94720

Synthesis, Characterization, and Ground Electronic State of the Unstable Monomeric Manganese(IV) Porphyrin Complexes Diazido- and Bis(isocyanato)(5,10,15,20-tetraphenylporphinato)manganese(IV). Crystal and Molecular Structure of the Bis(isocyanato) Complex

MARK J. CAMENZIND, FREDERICK J. HOLLANDER, and CRAIG L. HILL*

Received March 16, 1983

The complexes diazido(5,10,15,20-tetraphenylporphinato)manganese(IV), $Mn^{IV}TPP(N_3)_2$ (**1**), and bis(isocyanato)-(5,10,15,20-tetraphenylporphinato)manganese(IV), $Mn^{IV}TPP(NCO)_2$ (**2**), have been synthesized by reacting $Mn^{IV}TPP(OCH_3)_2$ with either trimethylsilyl azide or isocyanic acid (HNCO) at ~−50 °C. Both **1** and **2** are thermally unstable in solution at room temperature and decompose cleanly to $Mn^{III}TPP(X)$ (X = N_3 or NCO). Variable-temperature magnetic susceptibility measurements, EPR spectroscopy, UV/visible spectroscopy, and infrared spectra of **1** and **2** are distinct from those exhibited by formally isoelectronic Mn(III) tetraphenylporphyrin π cation radical complexes. The properties of **1** and **2** are consistent with a high-spin d^3 Mn(IV) ground electronic state. The infrared spectra of **1** and **2** show unusually low asymmetric stretching frequencies for the azide (ν = 1997 cm^{-1}) and isocyanate (ν = 2127 cm^{-1}) axial ligands. The complexes $Mn^{IV}TPP(X)_2$ (X = OCH_3, N_3, NCO) show highly anisotropic EPR spectra at 12 K that are consistent with a d^3 ion possessing a large zero-field splitting parameter, $|D| > 0.6$ cm^{-1}. Crystals of $Mn^{IV}TPP(NCO)_2 \cdot 0.5C_6H_5CH_3$ were subjected to X-ray crystallographic analysis. The complex crystallized in space group $C2/c$, with cell dimensions a = 21.200 (2) Å, b = 17.582 (2) Å, c = 21.999 (3) Å, β = 108.81 (1)°, V_{calcd} = 7762 (3) Å^3, and Z = 8. The structure was refined by least-squares techniques to a final value of R = 0.0408 (R_w = 0.0512) based on 3027 observations. The coordination about the manganese atom is pseudooctahedral with the average $Mn-N_{pyrrole}$ distance of 1.970 Å and the average $Mn-N_{NCO}$ distance of 1.926 Å. Although the $Mn-N_4$ unit is almost planar, the porphyrin core is distorted into a saddle shape by a large degree of quasi-S_4 ruffling. The average displacement of the meso carbon atoms from the N_4 plane is ±0.59 Å. The torsion angle of the two NCO ligands about the $N_{NCO(A)}-N_{NCO(B)}$ vector is 81.5°. The orientation of the NCO ligands and the ruffling of the porphyrin core can be attributed to crystal-packing forces.

Introduction

High-valent[1] manganese porphyrin complexes have been shown to be capable of oxidizing unactivated hydrocarbon C–H bonds to a variety of products in both stoichiometric and catalytic reactions,[2] and several manganese(IV) porphyrin complexes have recently been isolated from these systems.[3] Other high-valent manganese porphyrin complexes have been shown to be capable of evolving oxygen or hydrogen peroxide in thermal or photochemical reactions.[4] The isolation and determination of the structural and spectroscopic properties of a variety of high-valent manganese porphyrin complexes should greatly facilitate the study of their roles in these interesting reactions. Detailed spectroscopic studies of the complex $Mn^{IV}TPP(O_2)$[5,6] have been reported, and the isolation and X-ray crystallographic characterization of a monomeric Mn(IV)[7] and a monomeric Mn(V)[8] porphyrin complex have

* To whom correspondence should be addressed at the Department of Chemistry, Emory University, Atlanta, GA 30322.

(1) "High-valent" will be used in this paper to refer to manganese porphyrin complexes more oxidized than the manganese(III) porphyrin oxidation state, the stable oxidation state of manganese porphyrin complexes under aerobic conditions.

(2) (a) Smegal, J. A.; Hill, C. L. *J. Am. Chem. Soc.* **1983**, *105*, 3515. (b) Hill, C. L.; Smegal, J. A. *Nouv. J. Chim.* **1982**, *6*, 287. (c) Mansuy, D.; Bartoli, J.-F.; Momenteau, M. *Tetrahedron Lett.* **1982**, *23*, 2781. (d) Chang, C. K.; Ebina, F. *J. Chem. Soc., Chem. Commun.* **1981**, 778. (e) Mansuy, D.; Bartoli, J.-F.; Chottard, J.-C.; Lange, M. *Angew. Chem., Int. Ed. Engl.* **1980**, *19*, 909. (f) Hill, C. L.; Schardt, B. C. *J. Am. Chem. Soc.* **1980**, *102*, 6374. (g) Groves, J. T.; Kruper, W. J., Jr.; Haushalter, R. C. *Ibid.* **1980**, *102*, 6375. (h) Tabushi, I.; Koga, N. *Tetrahedron Lett.* **1979**, *38*, 3681.

(3) (a) Smegal, J. A.; Hill, C. L. *J. Am. Chem. Soc.* **1983**, *105*, 2920. (b) Schardt, B. C.; Hollander, F. J.; Hill, C. L. *Ibid.* **1982**, *104*, 3964. (c) Smegal, J. A.; Schardt, B. C.; Hill, C. L. *Ibid.* **1983**, *105*, 3510.

(4) (a) Harriman, A.; Porter, G. *J. Chem. Soc., Faraday Trans. 2* **1979**, *75*, 1543. (b) Porter, G. *Proc. R. Soc. London, Ser. A* **1978**, *362*, 281. (c) Tabushi, I.; Kojo, S. *Tetrahedron Lett.* **1975**, 305.

0020-1669/83/1322-3776$01.50/0